JOURNAL OF SPACECRAFT AND ROCKETS
Vol. 33, No. 3, May–June 1996

Experimental Verification of Interference-Free Testing Concept for Vehicles with Propulsive Jets

J. Olsson* and J. Agrell†
Aeronautical Research Institute of Sweden, S-16111 Bromma, Sweden
and
R. A. White‡ and H. H. Korst§
University of Illinois at Urbana–Champaign, Urbana, Illinois 61801

The results of an experimental investigation of the concept of interference-free testing using a cold-air modeled nozzle and flow-through sting are reported. A cold-air model nozzle ($\gamma = 1.4$) of a prototype propulsive rocket ($\gamma = 1.16$) from a previous study was used in conjunction with a streamtube shaped flow-through sting to examine the base pressure and separation for an 8 deg, $L/D = 1$ boattail due to the propulsive plume–slipstream interaction at a freestream Mach number of 2. Comparison to an extensive database for a strut mounted version of the same model and nozzle show that substantial improvements in pressure data quality result from the interference-free sting mounting and that the base pressure and flow separation location on the model are correctly simulated. The concept is shown to be applicable to the base pressure, as well as flow separation problems, and extend up to the 6-deg maximum angle of attack investigated.

Nomenclature

D = model centerbody diameter
M = Mach number
P = static pressures
P_0 = stagnation pressures
R = radius
R^* = nozzle throat radius
R_c^* = nozzle throat local radius of curvature
S = separation distance upstream from base plane
T_0 = stagnation tempratures
X = axial direction
α = angle of attack
β = boattail angle
γ = specific heat ratio
θ = angle between axial direction and local streamlines

Subscripts

b = base region
E = freestream conditions
F = expansion condition at nozzle exit
I = nozzle internal flow conditions
L = final wall point conditions at nozzle exit
M = model conditions
P = prototype conditions
S = plume surface

Introduction

THE difficulties in properly simulating the afterbody and base region pressures (and temperatures) on wind-tunnel models of rocket and jet propelled vehicles is well known. Numerous proposals for simulation parameters have been published,[1,2] although these have not produced satisfactory results as evidenced by the launch phase predictions for the Space Shuttle base drag. Indeed, new empirical correlations have recently been proposed.[3] Because of the complex nature of the slipstream-propulsive-jet interaction, which is exacerbated by the presence of control surfaces, boattails, and flares, this problem is not currently amenable to even advanced computational fluid dynamics (CFD) techniques. Approaches based on component models[4,5] that can only deal with simple afterbody configurations are excellent design tools but require some limited empirical input before being fully effective.

Consequently, for prototype performance prediction and CFD code confirmation wind-tunnel tests remain essential. The use of cold air for the propulsive jet in wind-tunnel testing is the most common procedure. In a series of earlier papers,[6–8] some of the authors have shown that the use of geometrically similar nozzles using cold air results in substantial errors in the base pressure and separation location for engine to freestream pressure ratios sufficient to cause separation on the afterbody; see Fig. 1 for the nomenclature. In other reports, Nyberg and Agrell[9] and Agrell and Gudmundson[10] have shown that other forms of plume simulation, such as solid bodies, are also unsatisfactory simulators of the exhaust plume.

In 1979 Korst and Deep[11] proposed that cold air ($\gamma = 1.4$) could be used to produce geometrically congruent plumes with pliability characteristics similar to that of the prototype ($\gamma = 1.16$), if the air nozzles were geometrically distorted and had a lower exit Mach number. This result was confirmed[6–9] in a series of experiments using gases of different specific heat ratio. The modeling and testing was done for both air to prototype propellant specific heat ratio and prototype propellant to air specific heat ratio (Fig. 2). These tests used the same wind-tunnel model and prototype nozzle as used

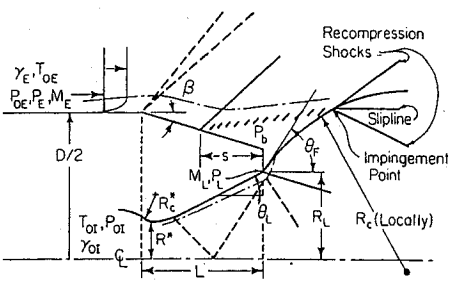

Fig. 1 Flow configuration for plume induced separation from conical afterbody.

Presented as Paper 94-2570 at the AIAA 18th Aerospace Ground Testing Conference, Colorado Springs, CO, June 20–23, 1994; received Aug. 15, 1994; revision received Aug. 3, 1995; accepted for publication Aug. 8, 1995.

*Research Engineer, High Speed Experimental Aerodynamics Department.
†Head, High Speed Experimental Aerodynamics Department. Member AIAA.
‡Professor, Mechanical Engineering. Associate Fellow AIAA.
§Professor Emeritus, Mechanical Engineering. Fellow AIAA.

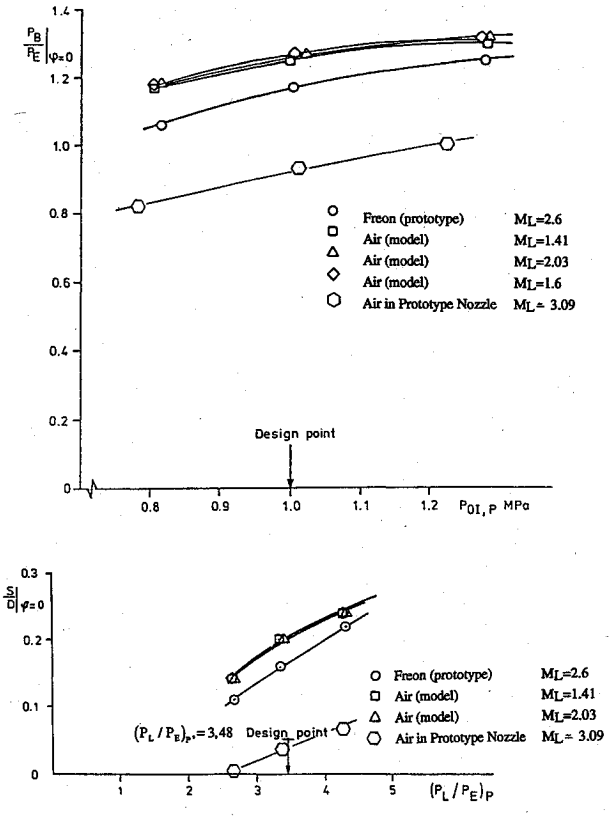

Fig. 2 Base pressure and separation distance for Freon (prototype) and (air model) nozzle: a) base pressure and b) separation distance.

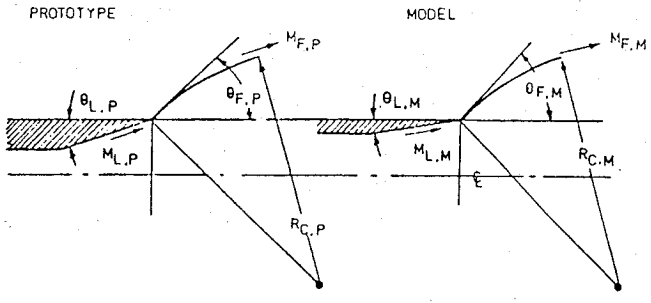

Fig. 3 Schematic of geometrical plume modeling from Ref. 15: $\gamma_P \neq \gamma_M$; $\theta_{F,P} = \theta_{F,M}$ and $R_{C,P} = R_{C,M}$ (two conditions).

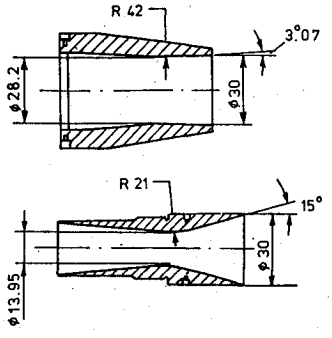

Fig. 4 Comparison of prototype and cold air model nozzle.

in an extensive test series[9] that included angle of attack, different freestream Mach numbers, control surfaces on the afterbody, and different length and angle boattails. Recently, the database formed by the tests of Refs. 5–9 was adopted by AGARD as a CFD test case.

Cold-air modeled nozzles[11] have a smaller exit Mach number and, consequently, larger throat area than typical rocket propellants ($\gamma_P < \gamma_M$). This suggests the possibility of using the larger throat cross section to pass a properly shaped flow-through sting of sufficient strength for complete model testing including angle of attack. Further, if properly designed, the sting-model combination should be interference free. This approach was used in Refs. 12–14 in a special series of tests with excellent results. The lack of a suitable comparative database and that the test series was not aimed at confirmation of the total concept, however, lead to the development of the special test program on which this paper reports. Thus, the objective of this investigation is to confirm that the combination of modeled cold-air nozzles in conjunction with a correctly shaped flow-through sting would result in correct base pressures, separation location, and influence of afterbodies, while being interference free. The tests were performed at a freestream Mach number of 2.0 and included the effects of angle of attack. The theory of interference-free testing using the model nozzle concept and specially shaped flow-through sting is reported in Ref. 15.

Concept and Design Choice

The basic concept of cold-air modeling of prototype nozzles has been discussed in several earlier papers.[5,7] The modeling methodology is such that the plume generated by the modeled nozzle has the same initial expansion angle at the nozzle lip (Fig. 3), the same curvature in the vicinity of the base plane, and a surface Mach number such that its pliability (at the confluence with the slipstream) is the same as that of the actual prototype plume. The resulting model nozzles have lower exit Mach numbers and exit plane lip angles (Fig. 4) that result in larger throat dimensions.

The larger throat area for $\gamma_M > \gamma_P$ can be sufficient to pass a flow through sting with the necessary strength to support the model under any anticipated loads. This configuration also allows for mounting a balance between the sting and the model so that force and moments can be measured directly. The presence of the sting must not, however, change the plume shape within the region downstream of the nozzle exit plane in which confluence with the slipstream will occur (Fig. 1). Since viscous effects are small due to the highly accelerated flow within the nozzle and plume at the nozzle lip, the presence of the sting should be negligible if the shape of the sting within the nozzle and for approximately one base diameter downstream is made to match the nozzle and jet flow streamlines.

The prototype nozzle selected was one that is typical of rocket propelled missiles and was tested as part of a verification study[5–9] of modeling from low-specific heat ratio ($\gamma = 1.16$) to high-specific heat ratio ($\gamma = 1.4$) air and from high-specific heat ratio air ($\gamma = 1.4$) to gas with a low-specific heat ratio ($\gamma = 1.16$). The dimensions and characteristics of the prototype nozzle and the cold-air model are shown in Fig. 4. Typical results comparing the performance of these nozzles from Ref. 9 are shown in Fig. 2. The agreement is seen to be good and also shows that using cold air through the prototype nozzle results in substantial errors in both base pressure and separation location.

Experimental Configuration

The original tests with the two nozzles were performed with a conventional strut-mount configuration as shown in Fig. 5. The propulsive jet gas was fed to the nozzle through the strut that was mounted as far forward on the model as possible to reduce interference effects on the afterbody and base region due to shocks and expansions from the mounting. Whereas interference effects were found to be small, even at angle of attack,[9] they were clearly present as seen in the pressure distribution variations on the afterbody (Fig. 6).

The flow-through sting installation is shown in Fig. 7 and has the advantage, assuming proper shaping of the sting contour, of being interference free in that no struts or mounts exist at any location on the test vehicle. The actual sting is one used in a previous test program at the FFA, Aeronautical Research Institute of Sweden to demonstrate the differences between plume simulation techniques.[10] For installation through the air model nozzle, $M_L = 1.41, \theta_L = 3.07$ deg (Fig. 4), the shape of the sting through the nozzle throat and expansion region (downstream of the exit plane where the influence of the lip expansion fan reflections from the sting will affect the plume) must be of the form of the flow streamlines.

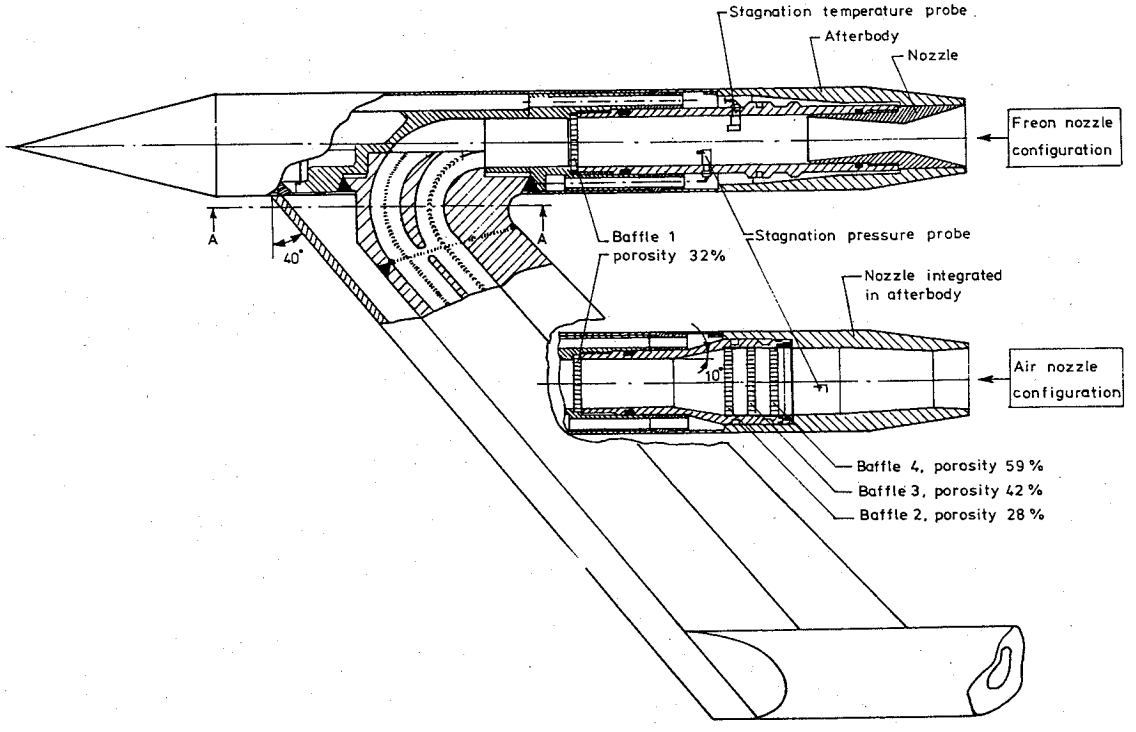

Fig. 5 Modified model II used in current modeling tests.

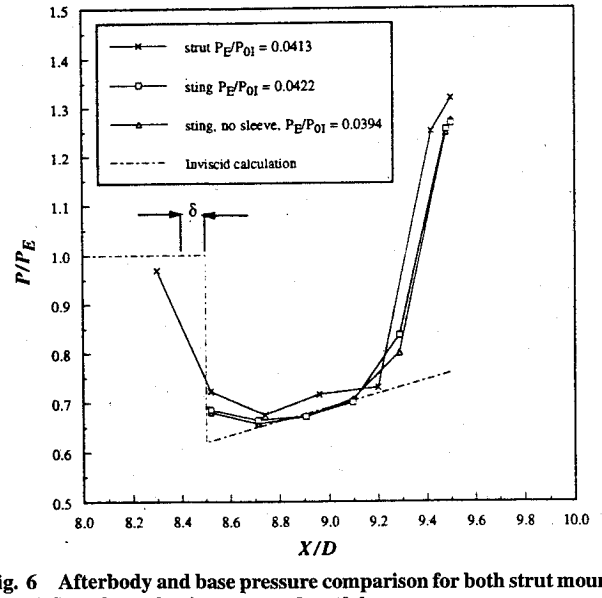

Fig. 6 Afterbody and base pressure comparison for both strut mounted and flow-through sting mounted model.

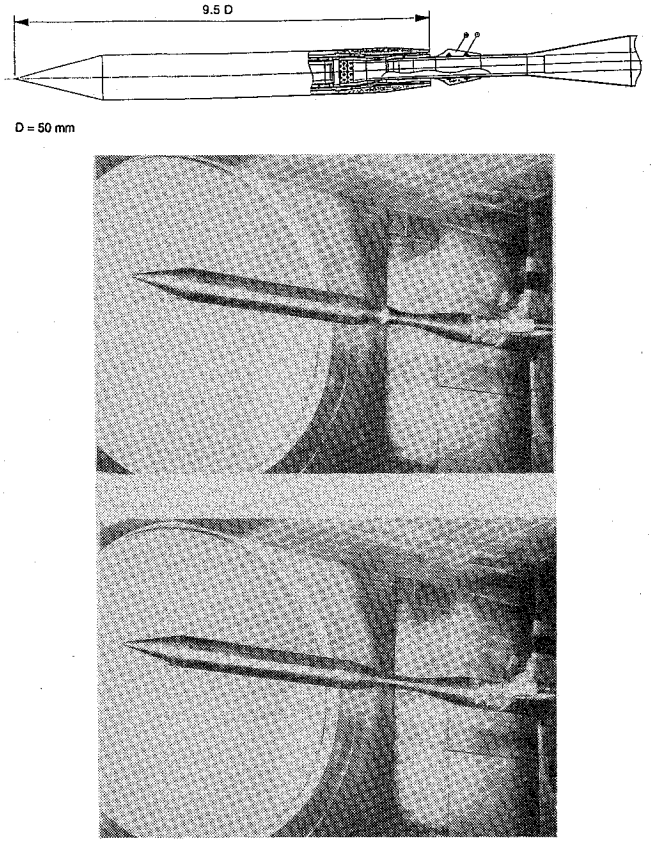

Fig. 7 Flow through sting details and photograph of the sting model installation with and without the sleeve.

Calculations of the streamlines within the nozzle and for the initial part of the plume, for a stream function of $\Psi = 0.65$, are shown in Fig. 8 for two different plume surface Mach numbers. Note that for higher engine-to-freestream-pressure ratios, i.e., higher plume surface Mach numbers, to obtain the proper plume shape it may be necessary to increase the sting diameter by the use of a sleeve starting approximately one body radius downstream of the nozzle base plane. The existing sting was modified by machining the surface to match the shape for the internal flow with $\Psi = 0.65$. A sleeve was manufactured, for the design point of the model nozzle, $(P_L/P_E)_P = 3.48$, and installed on the sting. Figure 7 is a photograph of the model and flow-through sting installation in the 0.5-m wind tunnel S5, at the FFA. This tunnel is of the suck down type and, consequently, the stagnation temperature and pressure are essentially atmospheric. The dew point is held at approximately −40°C by a silica-gel drying bed.

The missile body is the same as that used in Refs. 6–10 and consists of a 14-deg half-angle conical forebody and cylindrical centerbody with an 8 deg ($L/D = 1$) boattail. The model is 50 mm (1.97 in.) in diameter, and the overall L/D with the boattail is 9.5. The boattail is instrumented with six pressure taps located at $X/D = 8.52$, 8.712, 8.904, 9.096, 9.288, and 9.48, and the model was oriented with the taps at the zero meridian angle. An additional base pressure tap was located on the base halfway between the nozzle outlet ($R/R_{body} = 0.6$) and the final radius of the boattail at a meridial angle of 45 deg.

Table 1 Test matrix

($M_\infty = 2.0$)

Base pressure cases ← → base pressure and flow separation cases

P_E/P_{0_I}	Point design									
α	Jet-off	0.1202	0.0964	0.0806	0.069	0.051	0.040	0.036	0.027	0.017
0	X	X	X	X	X0	X0	X0	X0	X0	X0
±3 deg	0				X0	0	0	0	0	0
±6 deg	X0				X0	X0	X0	X0	X0	X0

X = without sleeve; 0 = with sleeve

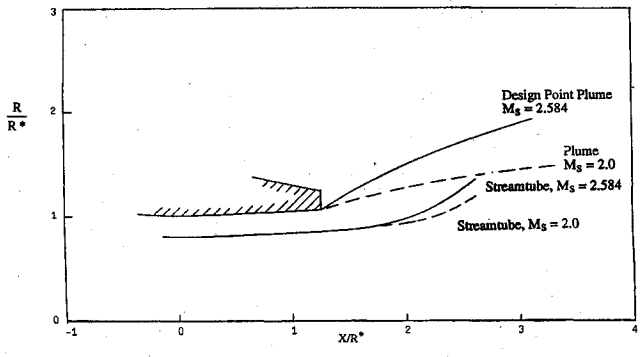

Fig. 8 Sting-streamtube shape for the point and an off design condition.

Test Program

The test program consisted of two parts. The first was a series of static tests, tunnel Mach number of 0, to check out the nozzle and the streamtube shaped sting. The nozzle was mounted on the model, but without the afterbody, and installed in the wind tunnel. The stagnation chamber door of the wind tunnel was kept closed allowing the test section to be evacuated to levels set by the vacuum system. This allowed the nozzle to be tested over a wide range of nozzle exit to adjacent pressure ratios to check the plume shape.

For these static tests the nozzle was instrumented with six internal pressure taps. One tap was located upstream of the nozzle throat, and the remaining five were located at equal spacing starting at the throat with the last being located as close to the nozzle exit as practical (approximately 0.01 X/D).

A dummy sting of the correct streamtube shape was mounted separately behind the model in a manner that allowed it to be inserted into the nozzle but with the capability to adjust its position both radically and axially. This installation permitted testing of the sting-nozzle combination to establish the sensitivity of the internal flow, determined by the internal pressure distribution, and the plume shape measured from schlieren photographs, to misalignment of the sting relative to the nozzle.

The second part of the experimental program consisted of a series of wind-tunnel tests at a freestream Mach number of 2.0. The test program included variations in nozzle to freestream pressure ratio and angle of attack. The test matrix used is summarized in Table 1. The range of pressure ratios included values reported in Refs. 6–9 for the strut mounted model. The test matrix, however, was expanded to include cases without afterbody separation (the base pressure case) and cases with increased separation on the afterbody. The influence of the sleeve was also studied by running part of the test matrix both with and without the sleeve installed.

Results and Discussion

The static tests were undertaken to determine the influence, if any, of the presence of the streamtube shaped sting on the internal (annular) flow in the nozzle. Figure 9 shows the calculated pressure distribution within and slightly upstream of the nozzle throat without the presence of the sting compared to the measured distribution with the sting in place. The agreement is excellent at all pressure ratios indicating that the presence of the sting does not affect the flow within the annular region of the nozzle. Only the last point near the exit plane is systematically low by approximately 0.01 P/P_{0_I}. A total error of less than 0.5 mm (0.02 in.) in the sting diameter at

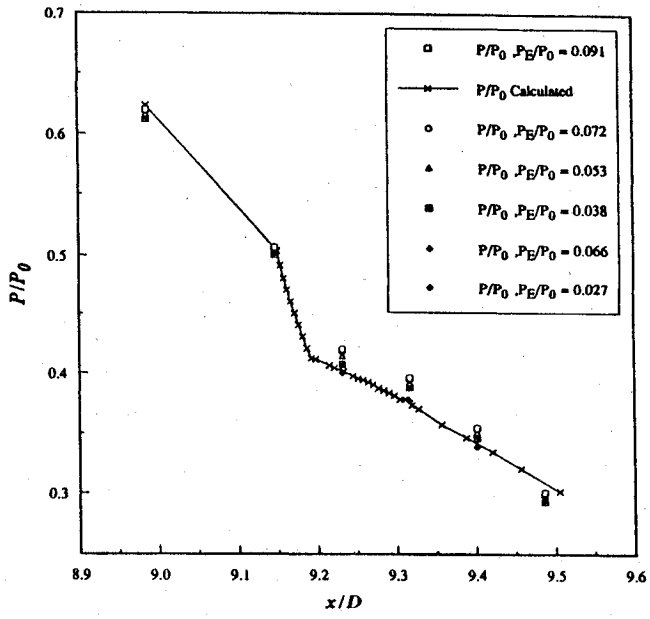

Fig. 9 Comparison of calculated and measure pressure distribution with the nozzles. Pressure in $M = 1.41$ nozzle with dummy string.

the exit plane, the nozzle exit diameter, and nozzle throat diameter combined changes the pressure distribution at that point by 0.03, which is greater than the measured difference. Further checks were made by translating the sting in the axial direction, ±0.5 mm (0.02 in.), which caused a change in the pressure ratio at an individual location by 0.025. The nozzle was also rotated 90 and 180 deg to check for concentricity, and no measurable change was found. Consequently, the dynamic tests were run with the nominal calculated sting position and consequent internal pressure distribution of Fig. 9.

Schlieren photographs of the plume were also taken and compared to the calculated prototype and modeled inviscid plume shape for a full flowing nozzle. The agreement was good in the range where interaction with the slip stream occurs.

The range of pressure ratios used in the dynamic tests, see Table 1, includes cases where no separation from the afterbody occurs, the base pressure sensitive problem, and extends to pressure ratios where separation exists for over 50% of the afterbody. In the latter cases the base pressure is no longer a sensitive indicator of the degree of plume–slipstream interaction due to the relatively small Mach number variation along the boattail caused by the decreasing radius and boundary layer (Fig. 6). The pressure rise at the separation shock is established by the free interaction concept,[16,17] which is only a function of the local freestream Mach number. Consequently, the base pressure becomes almost a constant at $P_b/P_E \sim 1.3$. Near the base plane, within approximately two to three boundary layer thicknesses, the pressure rise will be less than that predicted by the free interaction concept.[6–9] In this regime, however, the separation location on the afterbody is a strong function of the nozzle to freestream pressure ratio and is an excellent indicator of the correct modeling of the plume–slipstream interaction.

The separation point on the afterbody was determined in three ways for each run. They were (see Fig. 10) by 1) inspection of schlieren photographs for the shock location, 2) inference from the

afterbody pressure distribution, and 3) examination of surface oil-flow patterns.

Each method gave consistent and systematic results. Whereas the schlieren and pressure-distribution separation locations were in good agreement, the separation locations determined from the oil-flow pictures were consistently closer to the base plane, i.e., indicated less flow separation.

Figure 6 shows the afterbody and base pressure distributions for a case with $P_E/P_{0_I} = 0.042$ both with and without the sleeve installed. Results from a previous test series[9] using a hockey stick type of strut support are also shown (Fig. 5), along with an inviscid calculation of the afterbody pressure. The improvement in the pressure distribution over the afterbody due to the lack of interference from the strut is obvious. The flow-through sting data show little or no variation from the ideal inviscid calculated results except in the immediate vicinity of the intersection of the afterbody and centerbody where the boundary layer at the expansion smoothes out the inviscid discontinuity of the calculations.

The first test series were run at the design point $[(P_L/P_E)_P = 3.48]$ with the sleeve mounted on the sting. The pressure ratio was first varied over the range reported in Ref. 9. This range of pressure ratios restricted the base pressure to levels where flow separation was present in all tests. Subsequently, the range of the pressure ratios tested was expanded to that shown in Table 1. An examination of the results indicated that the flowfield near the design point and for larger jet to freestream pressure ratios was extremely sensitive to the sleeve shape forcing the afterbody separation location upstream. References 13 and 14 reported similar results. Consequently, the sleeve was removed, and the remainder of the tests were run without the sleeve installed.

Figures 11 and 12 show the base pressure and separation distances from the current study compared to the results of Ref. 9. Three significant features are immediately apparent in Fig. 11. First, the separation distances measured on the afterbody with the sleeve installed are in excellent agreement with the previous tests. The agreement with the Freon prototype is actually better than in the previous test series[9] for pressure ratios smaller than the design point, i.e., larger plumes, but are poor for the larger pressure ratios. In the latter cases the flow separates even for cases where no separation should occur. Second, with the sleeve removed the separation distances are in excellent agreement with the previous results for all test conditions. Third, the method of determining the separation location leads to a small but consistent difference. Previously reported differences[6–9] in separation location for the air models and Freon prototype may be due to differences in the measurement procedure, i.e., by schlieren photography or surface of oil-low patterns.

The base pressure shows the same effects of the presence of the sleeve, i.e., the base pressure is only in good agreement for nozzle

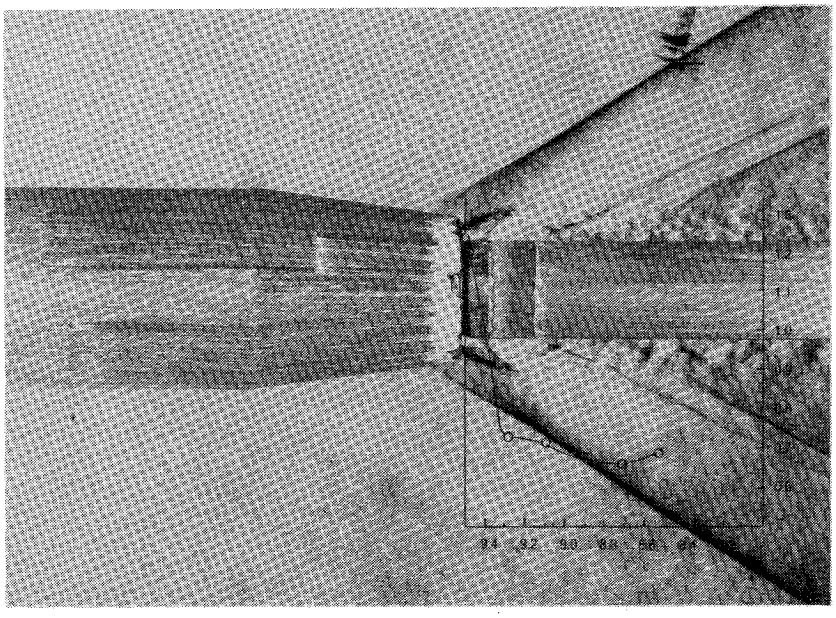

Fig. 10 Photograph montage of a schlieren picture, surface oil-flow pattern, and afterbody pressure distribution.

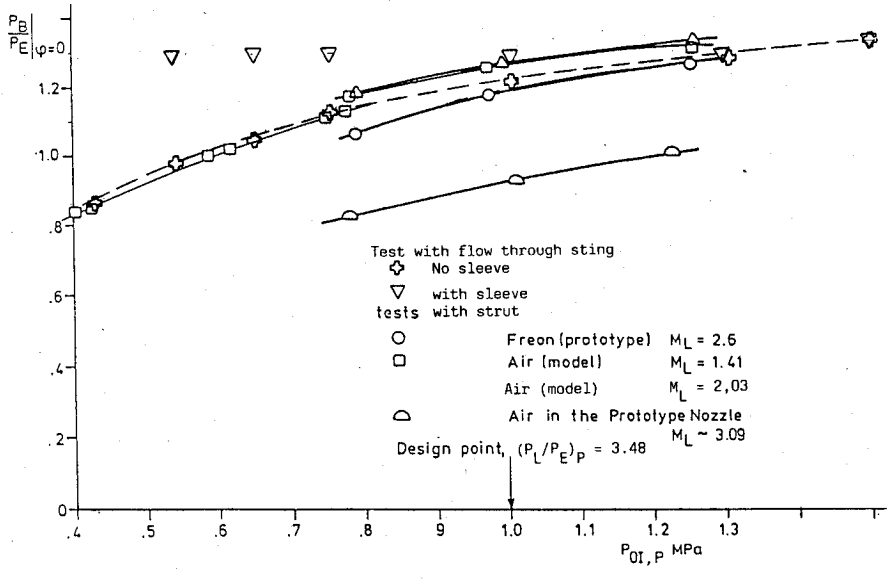

Fig. 11 Separation location for Freon and air nozzles with strut and flow-through sting.

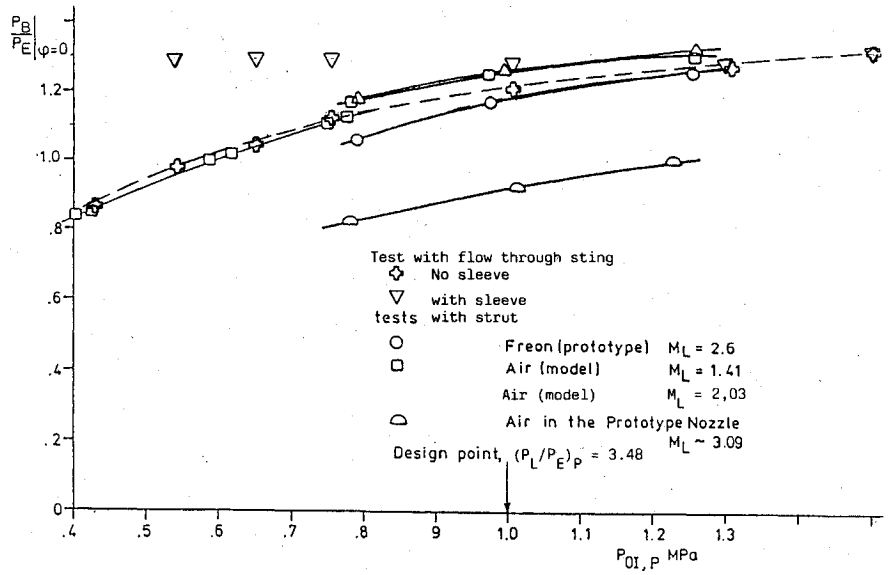

Fig. 12 Base pressure ratio for Freon and air in prototype plane.

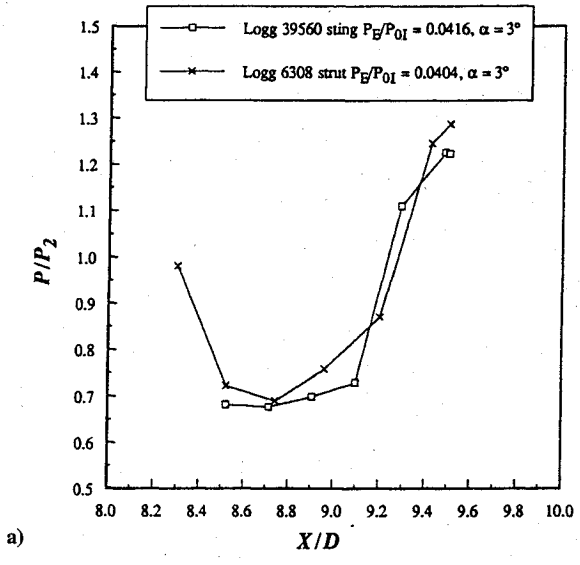

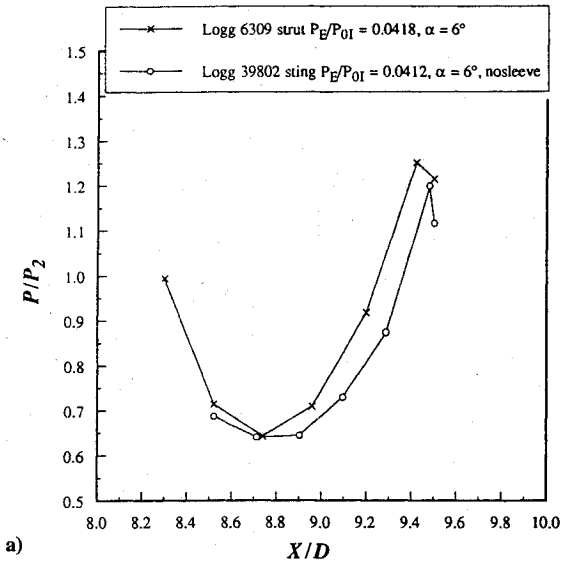

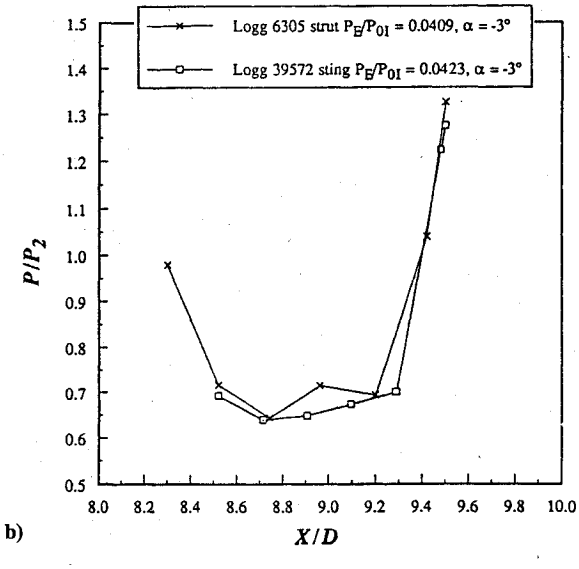

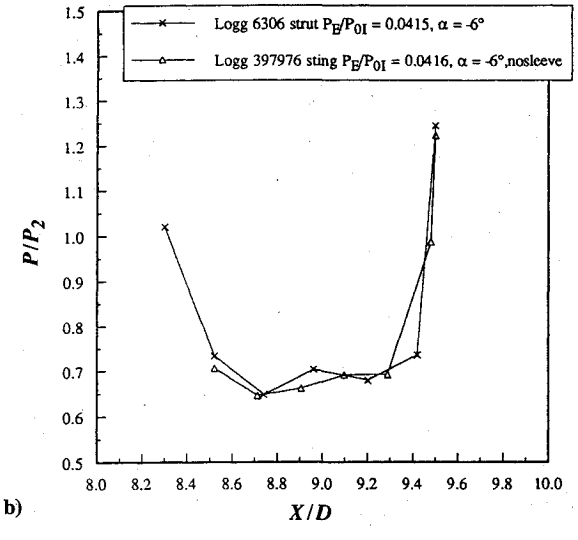

Fig. 13 Afterbody and base pressure comparison for the strut mounted and flow-through sting: a) $\alpha = 3$ deg and b) $\alpha = -3$ deg.

Fig. 14 Afterbody and base pressure distribution comparison for the strut mounted and flow-through sting: a) $\alpha = 6$ deg and b) $\alpha = -6$ deg.

pressure ratios less than the design point. With the sleeve removed, however, the base pressure is in excellent agreement over the entire test range including the base pressure cases where no separation occurs on the boattail. Figure 6 shows the afterbody and base pressure at a pressure ratio of $P_E/P_{0_f} = 0.042$, where the effect of the sleeve should be unimportant. The agreement between the two flow-through sting cases is very good with the strut mounted test showing the afterbody pressure nonuniformity referred to earlier and with a slightly earlier pressure rise at separation, indicating a slightly larger separation region.

As seen in Table 1, the first series of angle-of-attack tests were run with the sleeve in place. Similar to the zero-angle-of-attack cases the sleeve caused premature separation on the afterbody at the higher jet to freestream pressure ratios. Even for cases where the pressure ratio was smaller than the design point ratio the results were suspect, particularly at 6-deg positive angle of attack. The sleeve was removed, and the tests were rerun over a wider range of pressure ratios. The results at both plus and minus 3- and 6-deg angle of attack and all pressure ratios (Figs. 13 and 14) were in good agreement with the strut mounted configuration. The small differences are believed to be the result of the lack of interference from the strut that is more pronounced for the angle-of-attack cases.

Conclusions and Recommendations

The investigation shows that properly designed cold-air simulation nozzles allow the use of a flow-through sting that provides interference-free testing. The sting itself must be shaped to match streamtubes within the nozzle from the throat to slightly downstream of the nozzle exit plane so that the plume formed by the expanding nozzle flow at the nozzle lip has the correct surface Mach number, initial expansion angle, and curvature in the near (approximately 1 L/D downstream of the base plane) wake region. Within the range of variables tested, the program has established the merits and some limitations of the concept.

Specifically, the study has shown the following:

1) The quality of the pressure distribution data over the model afterbody is substantially improved, which demonstrates the interference-free nature of the flow.

2) The base pressure and separation location on the afterbody are in excellent agreement with previous test results using both cold air and Freon that showed that the sting's presence does not influence the plume and that the method provides proper simulation of the plume–slipstream interaction.

3) Based on the experiments, it appears that the sleeve designed to account for the influence of the expansion at the nozzle lip on the plume is not necessary, at least for the range of pressure ratios investigated in these tests.

4) The flowfield is very sensitive to the sleeve design even at the design point.

5) For the range of angles of attack investigated the influence of the sting is negligible.

It is recommended that experiments with an increased range of angle of attack and with control surfaces on the afterbody be undertaken to determine the limits imposed by the presence of the sting in the wake beyond that necessary to model only the near wake flow.

References

[1]Sims, J. L., and Blackwell, K. L., "Base Pressure Correlation Parameters," Workshop on Missile and Plume Interaction Flow Fields, Redstone Arsenal, AL, June 1977.

[2]Blackwell, K. L., and Hair, L. M., "Space Shuttle Afterbody Aerodynamics/Plume Simulation Data Summary," NASA TP 1384, Dec. 1978.

[3]Lamb, J. D., and Oberkampf, W. L., "A Review and Development of Correlations for Base Pressure and Base Heating in Supersonic Flow," Sandia National Lab., Sandia Rept. Sand 93-0280, VC-706, Albuquerque, NM, Nov. 1993.

[4]Korst, H. H., "A Theory for Base Pressure in Transonic and Supersonic Flow," *Journal of Applied Mechanics*, Vol. 23, No. 4, 1956, pp. 593–600.

[5]Korst, H. H., Chow, W. L., and Zumwalt, G. W., "Research on Transonic and Supersonic Flow of a Real Fluid at Abrupt Increases in Cross Section (with Special Consideration of Base Drag Problems)," Final Rept., ME-TR-392-5, Contract AF 18(600)-392, Univ. of Illinois, Urbana–Champaign, IL, Dec. 1959.

[6]White, R. A., and Agrell, J., "Boattail and Base Pressure Prediction Including Flow Separation from After-Bodies with a Centered Propulsive Jet and Supersonic External Flow at Small Angles of Attack," AIAA Paper 77-958, July 1977.

[7]Korst, H. H., White, R. A., Nyberg, S.-E., and Agrell, J., "Simulation and Modeling of Jet Plumes in Wind Tunnel Facilities," *Journal of Spacecraft and Rockets*, Vol. 18, No. 5, 1981, pp. 427–434.

[8]White, R. A., Agrell, J., and Nyberg, S.-E., "The Wind Tunnel Simulation of Propulsive Jets and their Modeling by Congruent Plumes Including Limits of Applicability," AIAA Paper 84-0232, Jan. 1984.

[9]Nyberg, S.-E., and Agrell, J., "Effects of Control Fins and Angle of Attack on Plume-Afterbody Flow Simulation," Aeronautical Research Inst. of Sweden, FFA AU-1763, 2nd ed., Stockholm, Sweden, 1986.

[10]Agrell, J., and Gudmundson, S. E., "A Review of the Experimental Technique Used at FFA in the Study of the Jet Effects on Afterbodies in Transonic and Supersonic Wind Tunnels and Some Results from the Investigations," Sitzung des DGLR-Fachausschusses, *Versuchswesen der Fluid- und Thermodynamik*, FFAP-A-370, Technische Universitet, Berlin, 1976, pp. 10–21.

[11]Korst, H. H., and Deep, R. A., "Modeling of Plume-Induced Interference Problems in Missile Aerodynamics," AIAA Paper 79-0362, Jan. 1979.

[12]Bernstein, D., and Fleener, W. A., "Plume Modeling and Analysis for High Altitude Flight," *Proceedings of the Symposium on Rocket/Plume Fluid Dynamic Interactions*, Vol. 1, *Base Flows*, Fluid Dynamics Labs. Rept. 83-101, College of Engineering, Univ. of Texas, Austin, TX, 1983, Sec. 6.

[13]Diamond, J. A., and Meldahl, K. R., "SRAM II Cold Plume Wind Tunnel Simulation Test Report (Series ED-1)," Vol. 1, Boeing Co., Seattle, WA, March 1990, p. 90.

[14]Diamond, J. A., and Meldahl, K. R., "SRAM II Cold Plume Wind Tunnel Simulation Test Report," Series ES-1, Vol. 1, Boeing Co., Seattle, WA, July 1990, p. 142.

[15]Korst, H. H., White, R. A., and Page, R. H., "Interferences-Free Wind Tunnel Testing of Jet Propelled Missiles Under Simulated Altitude and Full-Scale Reynolds Numbers," AIAA Paper 94-2567, June 1994.

[16]Mager, A., "On the Model of the Free Shock-Separated, Turbulent Boundary Layer," *Journal of the Aeronautical Sciences*, Vol. 23, Feb. 1956, pp. 181–184.

[17]Zukoski, E. E., "Turbulent Boundary Layer Separation in Front," *AIAA Journal*, Vol. 5, No. 10, 1967, pp. 1746–1753.

J. Allen
Associate Editor